JOURNAL OF MATERIALS SCIENCE 28 (1993) 4735–4743

Cyclic simple shear of metallic sheets: application to aluminium–lithium alloy

B. WACK, A. TOURABI
Laboratoire des Sols, Solides, Structures (formerly I.M.G.), BP 53 X, 38041 Grenoble Cedex, France

Plane shear tests without lateral force are obtained with the help of a very rigid shear device, attached to a classical testing machine. To avoid shear strain heterogeneity, essentially in the lateral direction, the shear strain is measured locally. The comparison with tensile test results indicates that for an elongation ratio of 10 the stress is determined with a systematic underestimate of about 4.5 %. This shear device allows extensive characterization of an aluminium–lithium alloy, available only in the shape of sheets: the shear modulus of tangential elastic behaviour, conventional yield strength, shear strength of asymptotic plastic behaviour, cyclic hardening and strength anisotropy can be determined. The accuracy of the test, due to the great rigidity of the apparatus, has also permitted determination of the lateral strain and consequently of a shear ratchet during cyclic loadings.

1. Introduction

The experimental study of the mechanical behaviour of metallic materials, which are only available in the shape of sheets, presents some difficulties. The sole test offering a zone of homogeneous state for stress and strain is the classical tensile test. But since the sample does not support any compression it is not possible to explore with cyclic tests some of the behaviour properties. Furthermore, due to the lateral contraction, a constriction instability appears rapidly and limits the behaviour study to small strain history; on the other hand, the industrial process of material forming indicates that the material may undergo very large strains. To increase the field of behaviour inspection a few less simple tests are sometimes used, like bending or sheet inflation, but the complexity of the tests renders it difficult to analyse these test results.

For these reasons it appears interesting to try to develop a plane shear testing method, as is done for solid polymers [1], the more so because the material is essentially submitted to a shear strain history in the industrial forming process. Large strains may probably be tested if buckling is avoided; furthermore the study of anisotropy seems *a priori* simpler than with tensile tests. Against this, the plane shear testing method presents some intrinsic defects proceeding from the limit conditions. On the one hand the clamping of the sample is certainly not perfect and some sliding will probably occur between the sample and the clamps. On the other hand the shear stress and strain vanish to zero at the two free ends, introducing then a heterogeneity in the stress and strain states. The aim of the present study also concerns the determination of these intrinsic defects.

In the present paper a description of the shear device is given, together with the general test conditions. Then the results of a series of low-cycle fatigue tests are analysed with regard to the shear modulus, the hardening phenomenon and the anisotropy. A comparison with tensile test results is made, allowing us to determine the limits of validity of the testing method. Finally the second-order effect of lateral strain is analysed and compared to the axial strain developed in torsion testing without axial force.

2. Experimental procedure

The shear of a plane sample is obtained with the help of a shear device, intended to be attached to a classical tensile testing machine, as suggested by two other studies [1, 2]. The shear device is essentially composed of a very rigid frame constituted by a rectangular box with a partial cover, inside which moves a vertical carriage. One sample clamp is bound to the frame and the other to the horizontal carriage (Fig. 1). Thus the device is able to impose a plane simple shear with no lateral force, similar to the simple torsion test of a tube without axial force [3].

To obtain a plane simple shear test as correctly as possible, and to particularly avoid undesired flexion, the frame and the carriages have heavy sections; thus the overall dimensions of the frame are approximately 390 mm × 320 mm × 100 mm for an allowed shear force of 25 kN (Fig. 2). Furthermore the relative motions are obtained by pairs of linear guides, symmetrically positioned with regard to the forces and of relatively great length, 300 and 180 mm for the vertical and the horizontal carriages, respectively. The linear guides are high-precision bearings of complementary M and V forms, with a double row of 5 mm diameter needles. This type of guide was chosen because of its ability to adjust the mechanical clearance, so as to approach the ideal situation of motion without friction and slack.

0022–2461

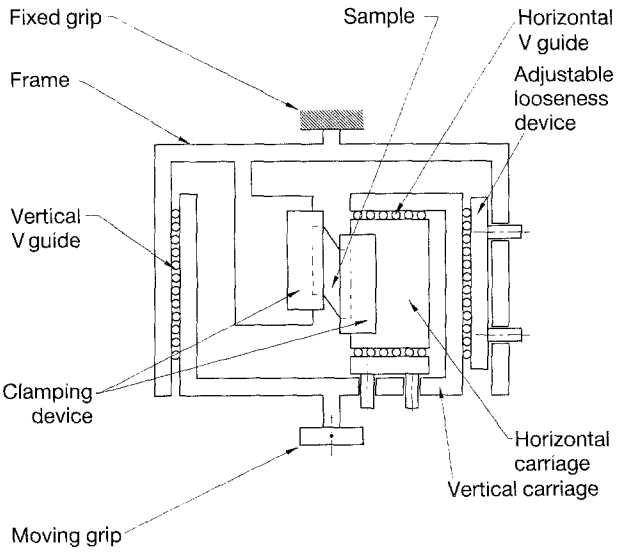

Figure 1 Scheme of the shear device.

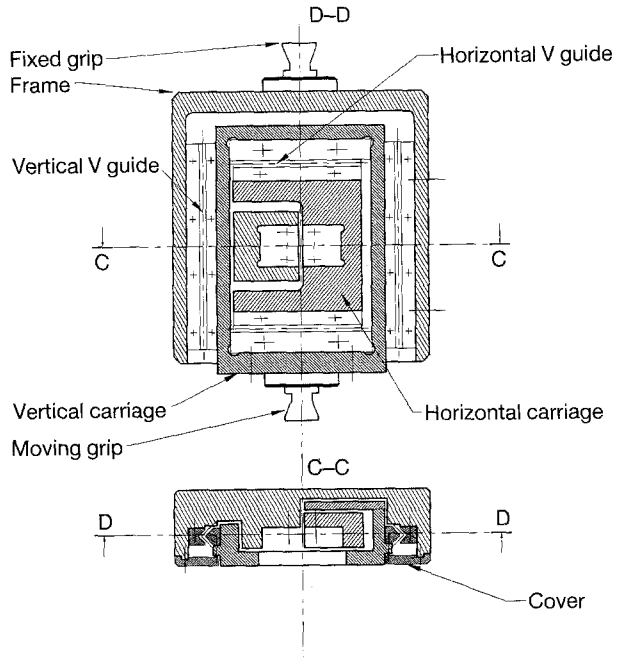

Figure 2 Detailed drawings of the main parts of the shear device.

The greatest sample height allowed by the shear device is 60 mm. The width of the sample sheared zone, i.e. theoretically the space between the edges of the two sample clamps, is adjustable due to the mobility of the horizontal carriage; its value is chosen with a view to satisfying two requirements: firstly the ratio l/e of the width to the thickness has to be small enough to avoid buckling of the sheared zone, and secondly the ratio H/l of the height to the width has to be great enough to minimize the error due to the non-homogeneity of the shear stress and strain at the two ends of the sample [1]. In our case the material sheet has a nominal thickness of 1.6 mm. We chose a height H of 50 mm and a width l of 5.0 mm, the overall dimensions of the sample being 50 mm × 22 mm (Fig. 3); these choices are made to optimize the stress range of the testing machine and to satisfy the preceding requirements.

To obtain a good shear strain measurement we use a local one. Indeed, in the lateral direction around the clamp edges, the decrease of the shear strain from the imposed value to zero does not happen abruptly, but in a strip of finite width. Therefore the measurement base for the relative displacement ΔZ of the two sample clamps differs from the theoretical value, i.e. the distance l between the two clamps; thus the direct measurement of ΔZ can give only a very rough strain measurement, which is always overestimated.

For most of the samples, the local strains are measured by a two-way extensometer, it was initially designed for axial and shear strain measurements of a tube-shaped sample with a 20 mm vertical base [4]. Thus some modifications were necessary: cranked iron needles of 1 mm diameter were used and the measurement base is given by the two diagonally opposite points of a rectangle of 10 mm height and 2.6 mm width (Fig. 3). The rectangle width is the measurement base b_y of the shear strain; it was chosen as great as possible, taking into account the theoretical shear zone width l and the diameter of the extensometer needles. The rectangle height b_z must not be too large, in order to reduce the error that disorientation of the sample may introduce. Assuming strain homogeneity in the reference rectangle ($b_y \times b_z$), the extensometer measures the variations dz and dy of the shear base b_y, thus determining the shear strain ε_{yz} and the lateral strain ε_{yy}:

$$\varepsilon_{yz} = \frac{1}{2}\left(\frac{dz}{b_y}\right) \qquad \varepsilon_{yy} = \frac{dy}{b_y}$$

For some samples the strains are measured by a strain-gauge rosette having a sensitive area of 3.5 mm × 1.0 mm (in that case the test number is followed by the symbol J).

The necessity for local strain measurement is fully justified by a comparison between the global axial relative displacement of the sample head Z_{gl} and the local strain measurement ε_{yz}, by extensometer or strain gauge. Typical results are displayed for symmetrical cyclic tests in Fig. 4. We see a significant hysteresis loop: it is due to sliding of the sample near the

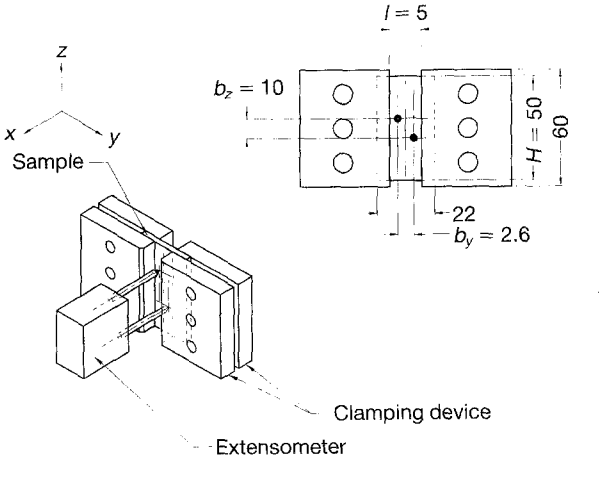

Figure 3 Geometry of the sample:- scheme of local strain measurement by the two-way extensometer. (Dimensions in mm).

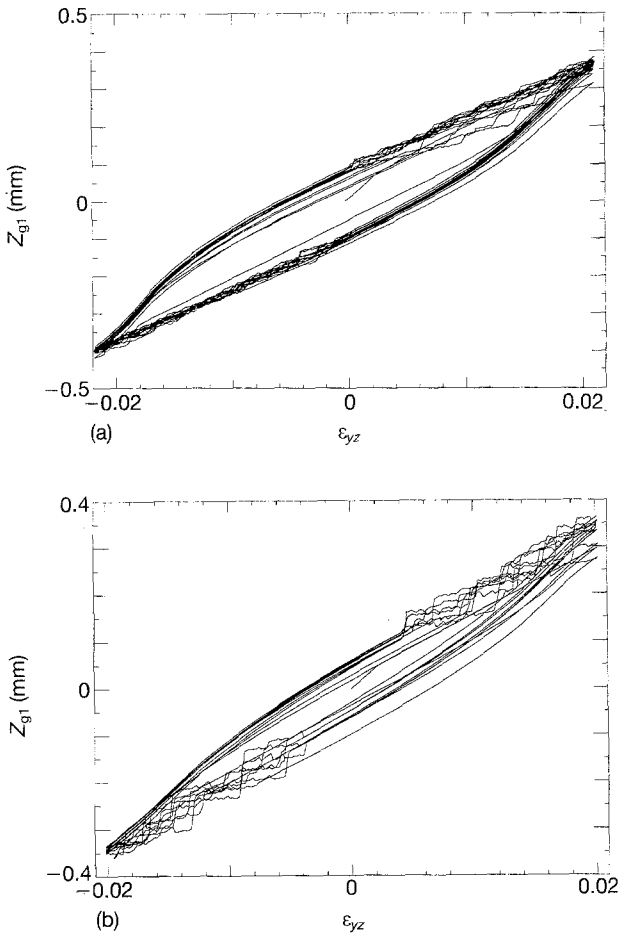

Figure 4 Comparison between the global axial displacement Z_{gl} of the sample head and the local strain ε_{yz} by (a) extensometer or (b) strain gauge symmetrical cyclic tests: (a) 0C3, $d_r = 24$ h, (b) 0A3, $d_r = 6$ h.

clamp edges. The ratio between the displacement rate and the shear strain rate evolves, along a loading branch, between a maximum value just after an inversion and a minimum mean value on the plateau of plasticity; the equivalent measurement bases for the global displacement are respectively 15 and 7 mm, values greater than the distance between the clamp edges (5 mm). Confirmation is given by observation of the marks left on the sample by the clamp striae: these marks are clearly bell-shaped over a distance of about 2 mm from the clamp edge. These results explain the difficulties encountered in correctly analysing this type of test, when a local strain measurement is not available.

The shear device is fitted with a counterweight. Thus, in addition to the mobility of the horizontal carriage, it is possible to clamp the sample without any stress. The sides of the sample are machined precisely, one side being used as reference, first for making slight marks for the extensometer needles and secondly for positioning the sample in the shear device.

The samples of the industrial 2091 aluminium alloy are obtained from 1.6 mm thick sheets elaborated by the Centre de Recherches de Voreppe (Pechiney) with a chemical composition given in Table I. After solution treatment (20 min at 527 °C), the material is water-quenched and strained 2 % to relieve internal stresses. The further thermal treatment is ageing at 150 °C for 6, 12 or 24 h. The grains are recrystallised and equiaxed with a diameter of 25 to 30 μm [5].

3. Results and discussion

3.1. Low-cycle fatigue shear tests

The tests are strain-controlled at a shear strain rate of 2×10^{-4} s^{-1}, with a shear strain amplitude of $\pm$ 2.0 % measured locally; the tests are stopped after the stabilization of hardening is reached (Fig. 5). The shear strain amplitude was chosen large enough to clearly reach the asymptotic plastic behaviour at the end of each loading branch. In addition to the influence of the ageing time ($d_r = 6$, 12 or 24 h), three directions of shear are tested, namely orientations 0, $\pi/4$ and $\pi/2$ with regard to the rolling direction, and denoted in the following by L, 45 and T respectively.

For these cyclic tests, some instabilities appear which can be classified in two types: they start almost systematically at the end of the second loading branch (first discharge branch); after an inversion, the instability phenomena stop and reappear on the quasi-plasticity plateau for all the following loading branches. The first type of instability, which gives small discharge cycles, is similar to those happening in the binary Al–Li alloys and is due to the shear and dissolution of precipitates in channels where the deformation is localized [6, 7]. The second type of instability giving small steps on the stress–strain plateau is the consequence of Portevin–Le Chatelier instabilities, which is another type of strain localization; these later instabilities are better revealed on a plot like Fig. 4, as will be explained and analysed in detail in a forthcoming paper. It has to be noted that the two types of instability do not appear when the strain amplitude is only $\pm$ 1 %, even after 30 cycles (Fig. 6).

The shear modulus μ is determined by separating the stress–strain curve in loading branches, starting at the origin or at an inversion state; the experimental data are transformed in the loading branch space by the coordinates

$$\Delta\varepsilon = \varepsilon - {}_R\varepsilon \qquad \Delta\sigma = \sigma - {}_R\sigma$$

where ${}_R\varepsilon$ and ${}_R\sigma$ are the reference coordinates of each loading branch, i.e. here the origin or the inversion state due to the simplicity of the loading history. The

TABLE I Chemical composition (wt %) of industrial 2091 aluminium–lithium alloy

Li	Cu	Mg	Zr	Ti	Si	Fe	Na	Al
2.0 ± 0.06	2.15 ± 0.06	1.58 ± 0.06	0.08 ± 0.003	0.02	0.04	< 0.05	0.0004	Bal.

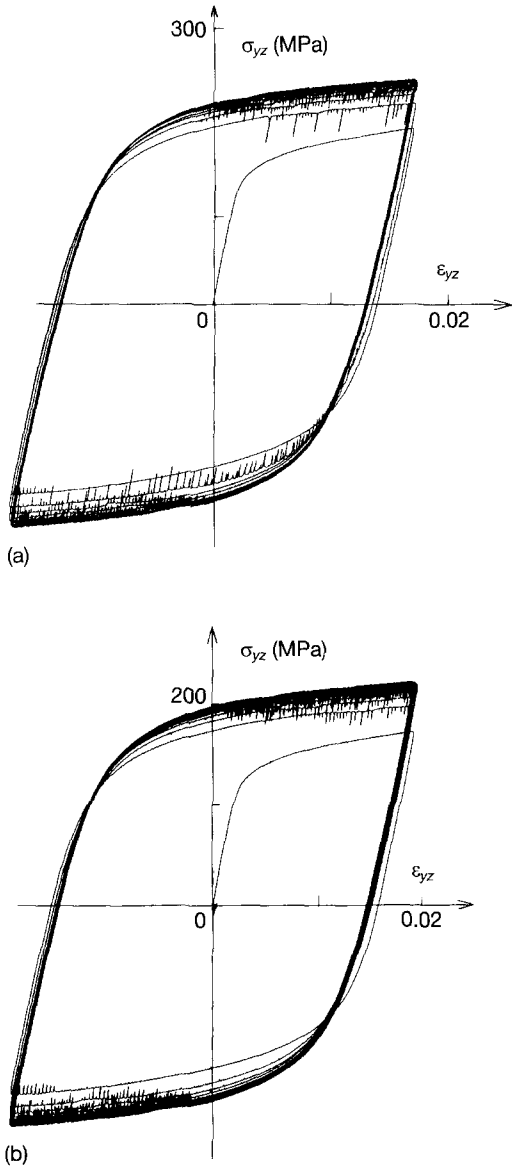

Figure 5 Typical results of cyclic shear tests: (a) 12 h ageing time and L direction (OB4), (b) 12 h ageing time and T direction (OB8).

slope M_μ is determined by a spline technique, its evolution being displayed versus $\Delta\varepsilon$. The shear modulus μ is the slope at the beginning of each loading branch; we have

$$M_\mu = \frac{1}{2}\left(\frac{d(\Delta\sigma_{yz})}{d(\Delta\varepsilon_{yz})}\right) = \frac{1}{2}\left(\frac{d\sigma_{yz}}{d\varepsilon_{yz}}\right) \qquad \mu = \lim_{\Delta\varepsilon \to 0} M_\mu$$

A typical result is given in Fig. 7. We see that the shear modulus μ_1 of the first loading branch is slightly greater than those of the other branches; this happens for all the shear tests and confirms the same property shown by the Young's modulus for tensile tests [8]. For that reason we determine for each test the shear modulus μ_1 of the first loading branch and the cyclic mean value μ_c of all the other branches (Table II).

As expected the results appear independent of the ageing time, but a slight influence of the direction exists, which has to be considered as a first manifestation of the material anisotropy. Table III reports, for the group L and T and the group 45, the mean values $\langle\mu_1\rangle$ and $\langle\mu_c\rangle$, as the standard deviation σ_μ of the

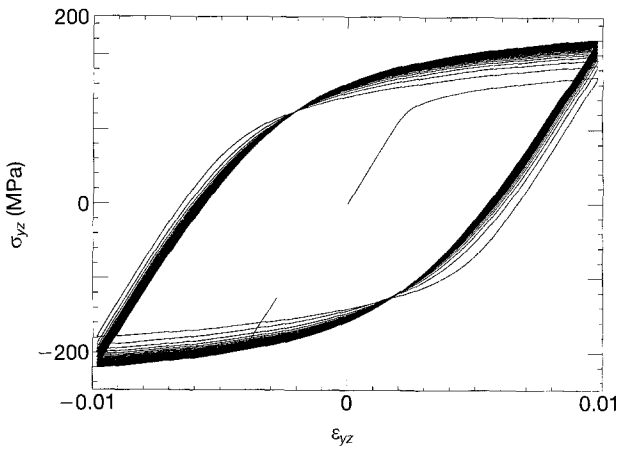

Figure 6 Cyclic shear test with small strain amplitude: the instabilities do not appear. 0A1, $d_r = 6$ h.

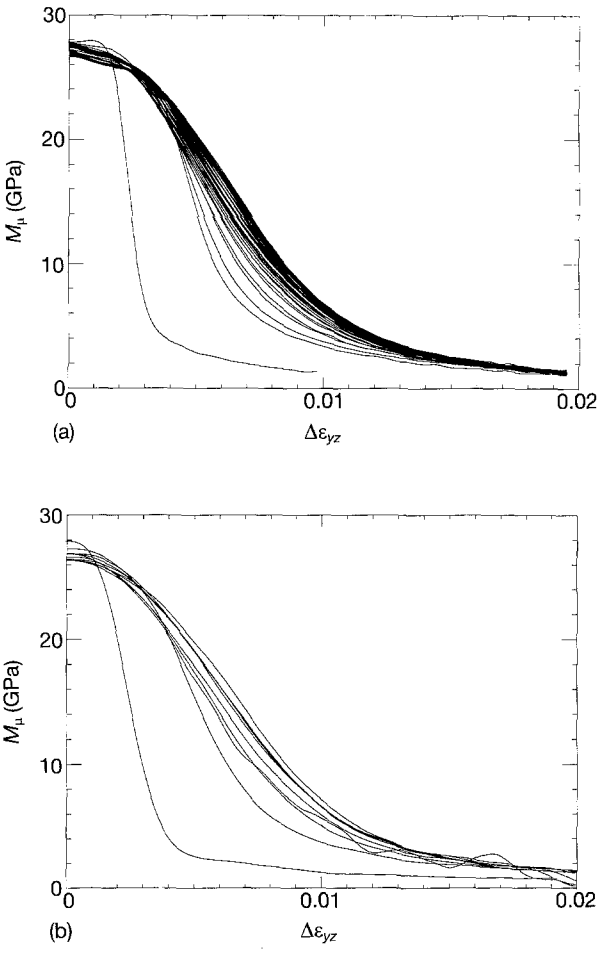

Figure 7 Modulus evolution versus the strain difference: (a) $\pm$ 1 % strain amplitude (OA1, $d_r = 6$ h), (b) $\pm$ 2 % strain amplitude (0B4, $d_r = 12$ h; only the beginnings of the curves are represented).

distribution of the n tests constituting a group and the standard deviation $\sigma_{\langle\mu\rangle}$ of the mean value of a group, assuming Poisson's law. For the directions L and T the ratio $\langle\mu_1\rangle/\langle\mu_c\rangle$ is equal to 1.041, i.e. a value almost equal to the value 1.038 found for the Young's modulus with the tensile tests, but for the direction 45 this ratio is only equal to 1.015. The anisotropy of μ_1 is almost insignificant; this result agrees with those obtained with resonant vibration techniques, the latter being systematically a little higher [9]. However, the

TABLE II Strength and shear modulus results

Test No.	Direction	Ageing time, d_r (h)	Strength (MPa)			Modulus (GPa)	
			R_{yz}	S^1_{yz}	S^M_{yz}	μ_1	μ_c
OA1-J	L	6	152	(171)[a]	(221)[a]	27.8	27.2
OA2	L	6	150	189	245	29.7	27.4
OA3-J	T	6	157	192	240	27.6	26.6
OA8	T	6	149	190	245	28.3	27.1
OB4	L	12	151	189	242	27.9	26.7
OB9	L	12	156	191	245	28.7	27.4
OB3	T	12	150	192	245	27.8	27.3
OB8	T	12	151	191	244	27.0	26.5
OC1	L	24	159	200	248	28.2	27.3
OC6	L	24	158	197	249	28.4	26.8
OC3	T	24	156	199	250	28.4	27.1
OC8	T	24	156	199	250	27.6	26.6
OD2-J	45	6	178	223	269	28.3	27.9
OE1	45	6	189	222	270	29.2	28.2
OD3	45	12	182	233	274	28.0	28.0
OE3	45	12	184	231	275	28.4	28.0
OD5	45	24	197	238	278	28.0	27.6
OE5	45	24	189	239	279	28.4	28.1

[a]The strain amplitude of test OA1-J is only $\pm$ 1 %.

TABLE III Statistics of shear modulus results

	L and T direction	45 direction
$\langle\mu_1\rangle$ (GPa)	28.12	28.38
σ_{μ_1} (GPa)	0.68	0.44
$\sigma_{\langle\mu_1\rangle}$ (GPa)	0.20	0.18
n	12	6
$\langle\mu_c\rangle$(GPa)	27.00	27.97
σ_{μ_c} (GPa)	0.34	0.21
$\sigma_{\langle\mu_c\rangle}$ (GPa)	0.10	0.08
n	12	6

anisotropy of μ_c is about 3.5 %, indicating that cyclic loading partially destroys the quasi-isotropy of the 2091 alloy, which is due to the recrystallized microstructure [10, 11].

The material strength is characterized first by R_{yz}, the classical strength at 0.2 % deformation determined from the tangential elastic behaviour. Secondly the asymptotic plastic strength is determined by the absolute stress value at the loading branch ends, i.e. S^1_{yz} for the first loading branch and S^M_{yz} after stabilization of hardening (Table II); a typical result for the evolution of S^i_{yz} with the number of loading branches is given in Fig. 8. As expected the strengths indicate, like the tensile strengths [8], an influence of ageing time and a marked anisotropy influence. By considering the two tests groups, L and T on one hand and 45 on the other hand, the results are analysed through a linear regression of the form

$$S_{yz} \text{ or } R_{yz} = aD_r + b$$

with

$$D_r = \log_{10}\frac{d_r}{6}/\log_{10}2$$

The results are summarized in Table IV; since the correlation coefficient r is small for some cases, we also indicate the strength average $\langle\rangle$.

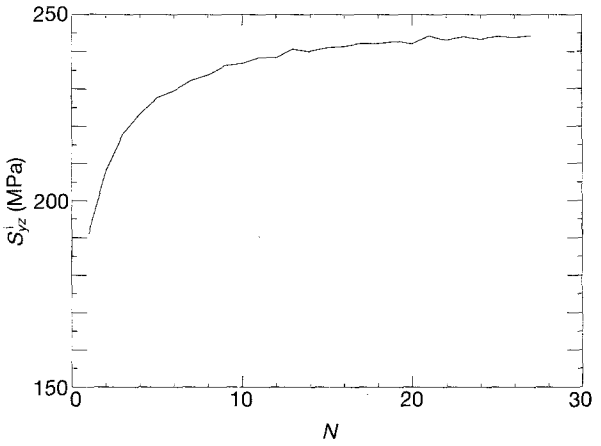

Figure 8 Typical evolution of S^i_{yz} versus the loading branch number N (0B8, d_r = 12 h).

The strength values indicate a clear material anisotropy due to the sheet rolling. For R_{yz} and S^1_{yz} the difference between L, T and 45 directions represents about 20 % of the L, T value; this difference decreases to 12 % for S^M_{yz}, the values for the direction 45 always being greater. It seems then that the cyclic test reduces the initial strength anisotropy, contrary to the initial elastic anisotropy (see above).

Finally the fatigue shear test also allows us to characterize the cyclic hardening phenomenon. In spite of the initial hardening due to precipitates, the cyclic hardening is still appreciable, as shown by the evolution of S^i_{yz} (Fig. 8 and Table II). For the directions L and T the ratio of the average values $\langle S^M_{yz}\rangle/\langle S^1_{yz}\rangle$ is equal to 1.27; for the direction 45 it is only equal to 1.19 (Table IV). This difference is consistent with the above-mentioned reduction of anisotropy due to cycling.

TABLE IV Linear regression analysis of shear test results

	L and T direction			45 direction		
	R_{yz}	S^1_{yz}	S^M_{yz}	R_{yz}	S^1_{yz}	S^M_{yz}
a (MPa)	2.63	4.41	3.08	4.75	8.00	4.50
b (MPa)	151.1	188.7	242.4	181.8	223.0	269.7
r	0.63	0.85	0.79	0.64	0.99	0.99
n	12	11	11	6	6	6
$\langle\rangle$ (MPa)	153.8	193.5	245.7	186.5	231.0	274.2

3.2. Comparison between tensile and shear tests

In order to discuss the validity of the shear test results it is of interest to compare them with those obtained with tensile tests. To a first approximation one may directly compare the tensile test results with the 45 direction shear test results, since the tensile test gives, on a smaller scale, local shear states oriented at about $\pi/4$ with regard to the tensile axis which is oriented parallel (L) or perpendicular (T) to the rolling direction.

The tensile tests are obtained with a classical shape of sample; the axial and lateral strains are locally measured by extensometer or strain gauges. For most cases, the loading history is constituted first by a loading until 2.5 %, followed by a few small cycles between 2.5 and 2.0 %, so that the tensile stress always remains positive; for these small strain-amplitude cycles hardening is of course negligible [8]. To respect the test axiality only orientations L and T are tested; most of the tests are conducted at a strain rate of 10^{-4} s^{-1}, and a few at 10^{-3} and 10^{-5} s^{-1}; as was the case for the shear tests, three ageing times are considered (6, 12 and 24 h).

The Young's modulus and the Poisson's ratio of the tangent elastic behaviour near the origin (initial value) or after an inversion (cyclic value) appear to be independent of the strain rate, the ageing time and the orientation. The average values of all the available test results are summarized in Table V. Following the preceding hypothesis, it is possible to determine the shear modulus for the 45 direction from the results of the tensile tests:

$$\mu^* = \frac{E}{2(1+\nu)}$$

We obtain for the initial and the cyclic states the following values:

$$\langle\mu_1^*\rangle = 29.98 \text{ GPa} \qquad \langle\mu_c^*\rangle = 29.01 \text{ GPa}.$$

It is interesting to introduce the ratio of the directly measured value to the value predicted from the tensile test; we have

$$\langle\mu_1\rangle/\langle\mu_1^*\rangle = 0.946 \qquad \langle\mu_c\rangle/\langle\mu_c^*\rangle = 0.964$$

It thus appears that the shear modulus obtained directly from the shear test results is systematically smaller than the value predicted from the tensile test, the relative mean error being 4.5 %. Since the strain is measured locally, this difference has to be explained by a systematic error in the shear stress determination,

TABLE V Young's modulus and Poisson's ratio from tensile test results

	Initial value	Cyclic value
$\langle E\rangle$ (GPa)	78.5	75.6
σ_E (GPa)	1.5	1.6
$\sigma_{\langle E\rangle}$ (GPa)	0.3	0.4
n	23	19
$\langle\nu\rangle$	0.309	0.303
σ_ν	0.010	0.008
$\sigma_{\langle\nu\rangle}$	0.002	0.002
n	21	18

TABLE VI Analysis of tensile tests at 10^{-4} s^{-1} strain rate

	T direction		L direction	
	R_{zz}	S^1_{zz}	R_{zz}	S^1_{zz}
a (MPa)	6.9	8.3	2.0	5.6
b (MPa)	330.4	413.0	344.0	401.1
r	0.73	0.76	0.47	0.82
n	9	9	5	5
$\langle\rangle$ (MPa)	338.1	422.2	345.2	404.4

as confirmed in the following by shear strength determination.

As for the shear tests, the tensile strength may be characterized by the classical strength R_{zz} at 0.2 % and by the stress at the end of the first loading branch S^1_{zz}. These values appear sensitive to the ageing time and the direction, and slightly to strain rate [8]. The results concerning the tests at 10^{-4} s^{-1} strain rate are summarized in Table VI and are to be compared with the results of Table IV for the 45 direction. Since the strain is large enough, the stress at the end of the cycle may be considered as a plastic limit stress. By assuming a Von Mises plastic limit surface we may determine, for the first loading branch only, the shear stress limit from the tensile stress limit:

$$S^{1*}_{yz} = \frac{S^1_{zz}}{3^{1/2}}$$

The comparison is made for the value obtained by linear regression at the middle ageing time 12 h, equal to $a + b$ (Tables IV and VI); for the tensile test results we consider the average of L and T directions; thus we have

$$\langle S^{1*}_{yz}\rangle = 239.0 \text{ MPa} \qquad \langle S^1_{yz}\rangle = 231.0 \text{ MPa}$$

which gives the ratio

$$\langle S^1_{yz}\rangle / \langle S^{1*}_{yz}\rangle = 0.966$$

We point out that the tensile strain and shear strain, respectively 2.5 and 2.0, are almost equivalent strains assuming a Von Mises plastic limit surface; thus the stress comparison remains valid despite the non-zero slope of the stress–strain curve at the end of the loading branch.

By assuming that the classical strength R is also described by a Von Mises surface and following the same averaging operation, we have

$$\langle R^*_{yz}\rangle = 197.3 \text{ MPa} \qquad \langle R_{yz}\rangle = 186.6 \text{ MPa}$$

with the following ratio:

$$\langle R_{yz}\rangle / \langle R^*_{yz}\rangle = 0.946$$

We see that the two ratio values obtained with the strengths are similar to those obtained with the moduli.

In conclusion, the comparison between tensile test results and shear test results indicates that we have to consider that the shear test apparatus introduces a systematic error underestimate of the shear stress of the order of 4.5 %. In fact, as mentioned earlier (in Section 2), the shear stress is not homogeneous at the two ends of the sheared strip, since the shear stress has to be exactly zero at the strip ends. For the geometry of our sample the equivalent height H_e of a homogeneous sheared strip would be 47.75 mm instead of the theoretical value of 50 mm. If we admit a linear variation of the shear stress at the two ends, from the zero value at the end to the constant value in the main part of the sample, we see that the two non-homogeneous zones have only a height of 2.25 mm, which is less than half of the sample width equal to 5 mm.

To reduce this error we may increase the elongation ratio H/l, i.e. increase the sample height or reduce the sample width. In the first case we are limited by the characteristics of the testing machine, as in the second case we are limited by the requirements of local strain measurement; thus the practical solution is a matter of compromise. Finally we also have to notice that this small systematic error may be neglected if we are only concerned with relative comparisons of shear test results.

3.3. Lateral deformation

A simple shear with no lateral force is also the occasion of a lateral deformation, which is a lengthening. This is a second-order effect of the shear, comparable to the axial deformation of a torsion test with no axial force [3]. This lateral deformation is small in comparison with the shear strain, but it is difficult to neglect it since this deformation accumulates during cyclic loading and thus is the occasion of a ratchet phenomenon.

The evolution of lateral deformation during cyclic shear tests is illustrated in Fig. 9, where results are given for the shear test with $\pm$ 1 % strain amplitude and an example of a shear test with $\pm$ 2 % strain amplitude. We notice that the first result is similar to the one given in Fig. 5 of Wack [3]. The lateral ratchet

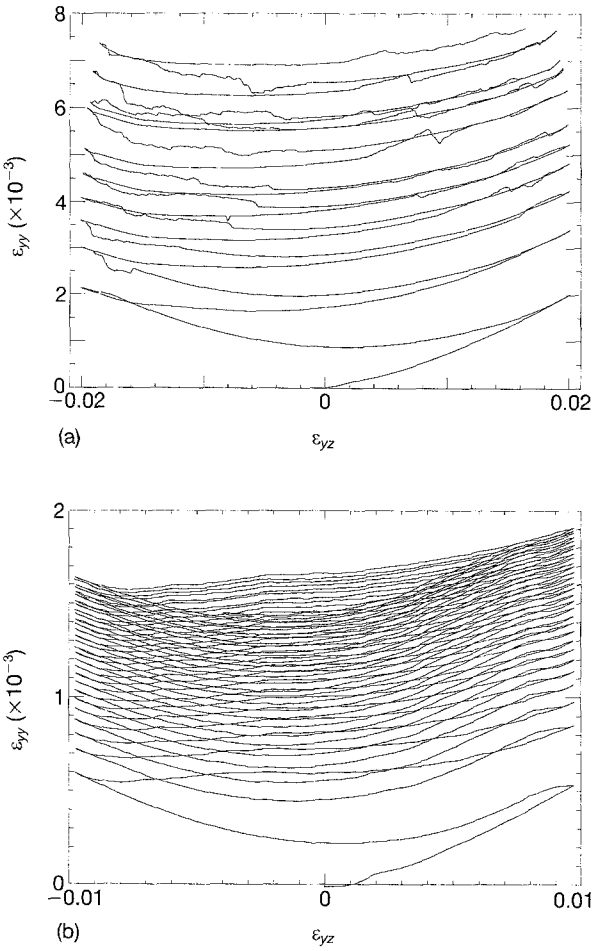

Figure 9 Typical evolutions of lateral deformation during cyclic tests: (a) 0D2, d_r = 6 h, (b) 0A1, d_r = 6 h.

evolution may be displayed by the evolution of the lateral strain ε_{yy} at the end of each loading branch versus the loading branch number N. A typical result is given in Fig. 10. The serrations which can be observed are due to a small asymmetry of lateral strain with regard to the shear strain sign (see for example Fig. 9).

The ratchet intensity may be characterized by the ratio K of the amount of ratchet per cycle to the shear strain amplitude per cycle. This ratio systematically diminishes with the number of cycles, from an initial value K_i defined by the first cycles, to a final value K_f defined at the end of the test (Table VII). Nevertheless for most tests a mean value K_m is significant, when for instance the ratio K_i/K_f is smaller than 2.5. Only two tests (0C1 and 0D2) show a constant K value during all the test, the ratios being respectively 8×10^{-3} and 14×10^{-3}; for two tests the lateral strain seems to stop after 7 (0C6) or 10 cycles (0C8).

The scatter of the results may be explained by the smallness of the strain: indeed the increase of lateral deformation is of the order of 0.4×10^{-3} per cycle, which corresponds to an increase of the measurement base of about 1 μm per cycle. At this level a few errors may then become non-negligible, as for instance the coupling between the two extensometer measures, or the play of the sample grips; furthermore the dispersion of the material characteristics may also be perceptible for this amount of strain.

TABLE VII Evolution of lateral deformation

Test No.	Direction	Ageing time, d_r (h)	K_m ($\times 10^{-3}$)	K_i ($\times 10^{-3}$)	K_f ($\times 10^{-3}$)
0A1-J	L	6	–	(5)[a]	(1)[a]
0A2	L	6	14	21	11
0A3-J	T	6	–	–	–
0A8	T	6	12	21	9
0B4	L	12	13	22	10
0B9	L	12	–	–	–
0B3	T	12	9	16	8
0B8	T	12	12	15	8
0C1	L	24	8	(8)	(8)
0C6	L	24	–	8	~0
0C3	T	24	–	34	9
0C8	T	24	–	17	2
0D2-J	45	6	14	(14)	(14)
0E1	45	6	–	30	5
0D3	45	12	16	23	13
0E3	45	12	14	23	10
0D5	45	24	11	21	9
0E5	45	24	23	32	18

[a]The strain amplitude of test OA1-J is only $\pm 1\%$.

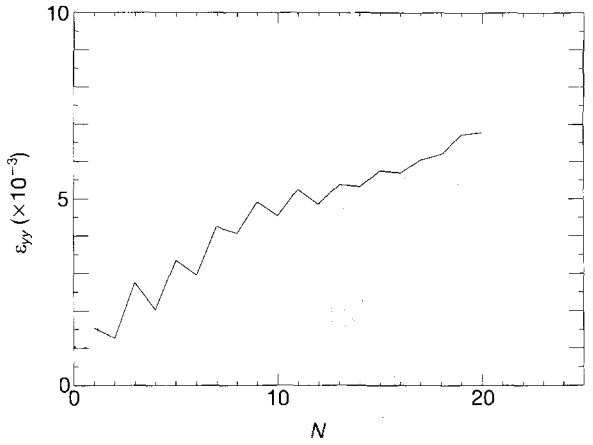

Figure 10 Typical evolution of the lateral ratchet versus the loading branch number (0B4, $d_r = 12$ h).

The quantity of results is not enough for us to analyse the influence of the ageing time or the orientation on this lateral ratchet. By supposing this influence negligible, it is possible to characterize statistically the series of nine results for which the ratio K_i/K_f is smaller than 2.5. Supposing a normal distribution, we determine the mean value $\langle X \rangle$ of K_m, K_i and K_f as well as the standard deviation σ_x of the individual values distribution and $\sigma_{\langle x \rangle}$ of the mean value distribution (Table VIII). Furthermore the theoretical distribution interval, with 95% confidence, is also indicated; the comparison of these interval limits with the experimental minimum and maximum values, namely X_m and X_M, indicates the validity of the preceding hypothesis.

The mean value K_m depends on the number of cycles, and the values of interest are the initial ratchet ratio K_i and the final ratchet ratio K_f which are material characteristics. The latter essentially determines the total amount of ratchet; its mean value (with 95% confidence) is

$$\langle K_f \rangle = (10.2 \pm 1.4) \times 10^{-3}$$

This value is much greater than those determined with torsion tests for a stainless steel, a superalloy and an engineering steel [3]. In spite of the difference between the two tests (the shear stress and strain are homogeneous in one case and not in the other case) this result seems to confirm the material dependence of the shear (or torsion) ratchet.

The initial value K_i is about double the final value; it only concerns about four cycles at the beginning of the test. Finally it has to be noted that this initial value does not take into account the lateral deformation corresponding to the first loading branch, whose value is relatively great (Figs 9 and 10).

These results suggest that there may exist a coupling between the evolution of the ratchet ratio (i.e. the ratchet increase per cycle) and the evolution of hardening: the initial high value K_i corresponds to the initial high hardening rate, as the final value K_f corresponds to the state when hardening is almost saturated for this imposed shear strain amplitude. Previous results concerning an axial ratchet accompanying cyclic torsion tests also reveal a decrease of the ratchet ratio with the number of cycles, but at that time only the

TABLE VIII Statistics of lateral deformation

	K_m ($\times 10^{-3}$)	K_i ($\times 10^{-3}$)	K_f ($\times 10^{-3}$)
X_m	9	14	8
X_M	16	23	14
$\langle X \rangle$	12.8	19.6	10.2
σ_x	2.0	3.5	2.1
$\sigma_{\langle x \rangle}$	0.7	1.2	0.7
$[.]_{0.95x}$	[8.8, 16.8]	[12.6, 26.6]	[6.0, 14.4]

mean ratio was studied with regard to the test conditions and the type of material [3]. This confirms the necessity to have an explanation, at the scale of the microstructural phenomena responsible for the deformation, to be able to analyse more precisely this ratchet phenomenon.

4. Concluding remarks

The experimental results obtained clearly show the interesting possibilities of this simple shear method as well as its limits of validity. The latter are essentially due to the fact that the frontiers of the sheared zone are not quite distinct: without particular care important errors may thus be introduced into the stress and strain measurements. Indeed the real width of the sheared zone varies during a cyclic test in a ratio of two between the quasi-elastic and the quasi-plastic states, and is always greater than the distance between the two clamp edges; for that reason the only solution for obtaining a valid shear strain measurement consists in a local strain measurement in the central part of the sheared zone. On the other hand, to minimize the error in the stress it is necessary to have a very elongated sheared zone, but nevertheless a systematic underestimation of the shear stress determination remains: for instance with a sample elongation ratio of 10 the shear stress is determined with a relative error of about 4.5 %, as determined by comparison with tensile tests results.

In spite of these defects this type of test presents important advantages for experimental investigations on materials available only in the shape of sheets. The sample form is very simple. The available results favourably complement those obtained with tensile tests, for instance for the determination of the rigidity moduli and the strengths. A precise study of the material anisotropy is also possible, the quality of the shear test being independent of the sample orientation, contrary to the tensile test. Furthermore the shear test allows a cyclic loading and therefore the study of cyclic hardening or softening phenomena. Finally the shear test of metallic sheets is tempting for engineers as well as for theoreticians. Indeed on one hand the shear test represents a better simulation of the real loading in the sheet-forming processes than is the case with the tensile test. On the other hand, the possibility of measuring the lateral strain may give sensitive information for the modelling of material behaviour, for instance concerning the definition of the reference frame.

Acknowledgement

The authors would like to thank the Pechiney Research Centre of Voreppe for providing the materials and for financial support through a contract.

References

1. C. G'SELL, S. BONI and S. SHRIVASTAVA, *J. Mater. Sci.* **18** (1983) 903.
2. E. F. RAUCH and J. -H. SCHMITT, *Mater. Sci. Eng.* **A113** (1989) 441.
3. B. WACK, *Acta Mech.* **80** (1989) 39.
4. A. TOURABI, thèse I.N.P.G., Grenoble (1988).
5. Ph. GOMIERO, thèse I.N.P.G., Grenoble (1990).
6. Y. BRECHET, S. HAN, F. LOUCHET and B. WACK, in "Comportement en fatigue de torsion de l'alliage binaire aluminium–lithium. Aspect macroscopique et microstructure" (Report L.T.P.C.M. and I.M.G., Grenoble, 1986).
7. Y. BRECHET, thèse I.N.P.G., Grenoble (1987).
8. B. WACK and A. TOURABI, in "Etude des propriétés mécaniques de l'alliage industriel 2091" (Report I.M.G., Grenoble, 1990).
9. W. D. ROONEY, J. M. PAPAZIAN, E. S. BALMUTH, R. C. DAVIS and P. N. ADLER, in Proceedings of 5th International Aluminium–Lithium Conference, Williamsburg, VI, March 1989, edited by T. H. Sanders and E. A. Starke (Materials and Component Engineering Publications Ltd, Birmingham, 1989) p. 799.
10. P. MEYER and B. DUBOST, in Proceedings of 3rd International Aluminium–Lithium Conference, Oxford, July 1985, edited by C. Baker, P. J. Gregson, S. J. Harris and C. J. Peel (Institute of Metals, London, 1986) p. 37.
11. P. MEYER, Y. CANS, D. FERTON and M. REBOUL, in Proceedings of 4th International Aluminium–Lithium Conference, Paris, June 1987, edited by G. Champier, B. Dubost, D. Miannay and L. Sabetay (Editions de Physique, Paris, 1987) p. C3-131.

Received 12 June 1992
and accepted 1 January 1993